Proceedings of the 5th International Conference on Materials Chemistry and Environmental Engineering
DOI: 10.54254/2755-2721/2025.29501

Non-Fluorinated Durable Water Repellent (DWR) and Stain-Resistant Coatings

Zizhen Lei[1*†], Yueru Li[2†], Yuanbin Wang[3]

[1]*School of Chemistry and Molecular Engineering, East China University of Science and Technology, Shanghai, China*
[2]*School of Materials Science & Engineering, Shandong University, Jinan, China*
[3]*Tabor Academy, Marion, USA*
**Corresponding Author. Email: aidenlei2003@gmail.com*
[†]*These authors contributed equally to this work and should be considered as co-first author.*

Abstract. Fluorinated materials are used in stain-resistant coatings in fields like buildings and pipelines. However, due to their poisonousness and biopersistence, fluorinated materials harm both human health and the environment, and they cannot be widely used due to high prices. Researchers are trying to develop non-fluorinated materials that could have equal characteristics while being cheaper and more eco-friendly. People often learn from nature, drawing inspiration from creatures' ability to stay clean. Inspired by these natural phenomena, readers would have a better grasp of how to develop non-fluorinated hydrophobic materials. In addition to basic theatrical backgrounds, this article also provides a comprehensive overview of the synthesis methods, material selection, and application prospects of non-fluorinated superhydrophobic and stain-resistant materials, and introduces four methods for preparing non-fluorinated superhydrophobic and stain-resistant materials. Each method has its own distinct advantages and limitations, which make them suitable for different application scenarios. Commonly used materials include silicone, organic, and inorganic materials, each with distinct properties and a range of applications.

Keywords: non-fluorinated materials, stain-resistance, coating, durable water-repellent

1. Introduction

1.1. Definitions and applications

1.1.1. Fluorinated materials

Fluorinated materials have a long history of utilization within a number of different sectors, including textiles, footwear, tents, biomedical devices and other biomaterials. Such materials are typically carbon-based polymers containing considerable amounts of fluorine that is chemically bonded to the polymer backbone. Their physical state may be solid, liquid, thin film, coating, or gel, depending on the chemical composition, processing, and intended application.

© 2025 The Authors. This is an open access article distributed under the terms of the Creative Commons Attribution License 4.0 (https://creativecommons.org/licenses/by/4.0/).

DOI: 10.54254/2755-2721/2025.29501

Fluorinated polymers exhibit a range of distinctive properties, including chemical inertness, exceptional hydrophobicity and solvent resistance, low coefficients of friction, high design tolerances for device fabrication, and temperature resistance. These properties permit their utilizations in specific technologies where the majority of other hydrocarbon-based materials are unable to perform adequately, such as in the manufacture of devices [1].

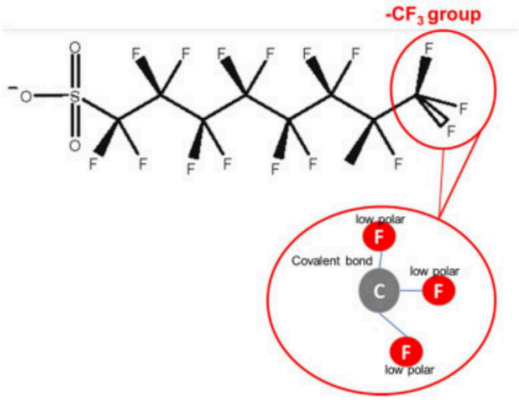

Figure 1. Perfluorinated compound basic structure [2]

Perfluorinated compounds (PFCs) are macromolecules containing -CF, $-CF_2$ and $-CF_3$ in the backbone, as shown in Figure 1. The $-CF_3$ group has the lowest surface energy of any known small molecule group. This low surface energy is a direct result of the electronegativity of fluorine and its very small van der Waals radius (147 p.m.).

1.1.2. Stain-resistance

The resistance to contamination by solid, liquid and semi-liquid particles is the stain resistance. Typical ways to make a surface stain resistant include the use of various types of coatings, sealants or films. Self-cleaning surfaces are also a part of the stain-resisting material family. Such surfaces are typically developed by combining low surface energy and texture [3].

1.2. Hazards of fluorinated materials

1.2.1. Harmful health effects

The two best known and most studied fluorinated compounds are perfluorooctanoic acid (PFOA) and perfluorooctanesulfonic acid (PFOS) - both of them are well known to cause adverse health effects. Despite fluorine representing the 24th most abundant element in the universe and the 13th most abundant element in the Earth's crust, it can be considered to have no presence in the biosphere [4]. Skeletal fluorosis can be caused by eating, drinking or breathing very large amounts of fluoride. But don't worry too much, this condition only occurs after long-term exposure and can cause denser bones, joint pain and limited joint movement. Although almost half of the fluoride ingested is rapidly stored in hard tissues, it will take much longer to get released. Today, increasing use of polyfluoroalkyl substances, fluorinated medicines and fluorinated agrochemicals may indirectly lead to potential risks. To illustrate, the metabolism of fluorinated compounds can result in the production of toxic fluorine-containing metabolites (such as fluoride or fluoroacetate), which may result in elevated fluoride concentrations in body fluids and tissues [4].

DOI: 10.54254/2755-2721/2025.29501

It can also cause liver and thyroid disorders, immune dysfunction, various types of cancer, high cholesterol, birth defects and infertility [5].

1.2.2. Biopersistence and degradation

Because of carbon–fluorine bonds, one of the strongest bonds found in nature, these synthetic compounds are able to withstand extremely harsh environmental conditions and typical natural forces of degradation (sunlight, enzymes and bacteria) are unable to break this strong bond. As a consequence, the half-life of PFOA is > 90 years, and the half-life for PFOS is > 40 years [5].

In essence, all PFASs are manufactured via one of two principal production pathways: electrochemical fluorination (ECF) and topomerization [6]. The two production pathways employ a basic material, also designated Telomer A, along with a series of replacement reactions to yield a vast spectrum of fluorotelomer-based PFASs. The production of fluorotelomers is accomplished through a series of substitution reactions, which renders them susceptible to further chemical transformations and degradation within the natural environment, leading to the formation of other PFAS compounds. The Stockholm Convention's listing of PFOA under Annex A (banned) was prompted by concerns over the degradation products of PFOA-related substances [7].

1.2.3. Expensive costs

Furthermore, the high cost of fluorinated compounds and the complexity of the fluorination process may impede the large-scale utilization of these compounds in industry. Taking PDMS and PTFE as a comparison, the average price for the former one is about $3000 per ton (Purity: 99%; Brand: DOBO), while the average price for the latter one is about $13,000 per ton, and details prices for PTFE in different countries are showed in the Table 1.

Table 1. PTFE Prices in USD / metric ton [8]

	Q4 2023	Q3 2023
PTFE, US	15,500	14,700
PTFE, EUR	17,300	17,200
PTFE, SEA	11,500	12,700
PTFE, CN	8,650	7,970

1.3. Non-fluorinated durable water repellent (DWR)

Given all of the challenges associated with the use of fluorinated materials, there has been a significant recent push to look for non-fluorinated alternatives for utilization as DWR fabric coatings.

1.3.1. Advantages

It can be posited that non-fluorinated DWRs could potentially be utilized in textile products that only necessitate effective water repellency for the duration of their product lifetime. However, a niche market may persist for textile products that require not only high oil/stain repellency but also durability. Nevertheless, it may be more crucial to prioritize the mitigation of the risks associated with the release of highly persistent chemicals into the environment.

DOI: 10.54254/2755-2721/2025.29501

1.3.2. Disadvantages

It is difficult to achieve oleophobic properties without the use of fluorinated materials and/or specific surface structures and coating processes, which may limit their replacement potential in textile applications requiring oil repellence [9].

Today, researchers have coated various substrates with non-fluorinated membranes (polydopamine and polyethylene polyamine) to make them more hydrophilic and oleophobic, but this process takes about two days to process, which limits its application on an industrial scale and at a low cost [2].

1.4. Challenges with non-fluorinated materials

A significant challenge associated with non-fluorinated superhydrophobic coatings is the inherent fragility of the infused nanoparticles within the coating films, which can potentially compromise their non-wetting properties [10]. The mechanical durability of a surface is dependent upon a number of factors, with the strength of the bonding between the surface and the water-repellent coating being of particular consequence. The mechanical durability of SiO_2/polymer blocks has been evaluated, and the results are presented in Fig. 2 [9]. It was observed that WSA (water sliding angle) and WCA (water contact angle) declined significantly after abrasion, indicating that the surface was unable to retain its superhydrophobic properties. Additionally, other parameters, such as oleophobicity, were also found to be unsatisfactory [3].

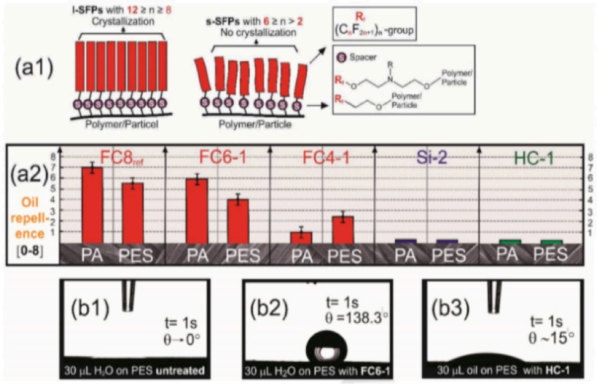

Figure 2. (a1) Side-chain orientation of SFPs, (a2) Oil resistance measurement results and different wettability of mineral oil to (b1) surface of untreated PES, (b2) surface of C8 L-SFP, and (b3) surface of hydrocarbon DWR, showing no hydrophobicity, superhydrophobicity, and low oleophobicity, respectively [9]



Figure 3. Compared WCA and WSA of initial and after abrasion [3]

DOI: 10.54254/2755-2721/2025.29501

1.5. Scope of the article

This article details the theoretical background such as contact angle, young's relation and basic models of Wenzel and CassieBaxter models. Natural phenomena like lotus leaves and water striders' ability to help them stay clean are also introduced. In addition, this article describes four methods for preparing non-fluorinated superhydrophobic and stain-resistant materials, including etching and lithography techniques, layer-by-layer (LBL) assembly, electrochemical reaction and deposition, and colloidal templating, each with distinct properties and range of applications. Commonly used three materials (silicone, organic, and inorganic materials), aiming to contribute to the development of a new generation of non-fluorinated DWR coatings and materials.

2. Theoretical Background

Before learning about specific examples and applications of fluorinated and nonfluorinated hydrophobic surfaces, theoretical background such as contact angle, young's relation and basic models of wenzel and cassie baxter models are important knowledge to learn about. Contact angle and surface tensions are properties of surfaces that determine whether they are hydrophobic or hydrophilic. Wenzel and cassie baxter models introduce two different ways of water and surface contact. Through introduction of non-fluorinated hydrophobic materials, readers would have a better grasp of why we should develop non-fluorinated hydrophobic materials.

2.1. Contact angle and Young's relation

The angle formed when the droplet is in contact with the solid surface, that is, the contact angle, can be determined by measuring the angle between the tangential line between the droplet and the solid surface. The measurement of the contact angle θ has the advantage that it can be performed relatively easily on a properly treated solid surface to estimate the tension between the solid-vapor and solid-liquid interfaces.

The discovery of estimating the surface energy of a solid from the contact angle relies largely on the principle proposed by Young in 1805. On a solid surface, the contact angle of the droplet is determined by the mechanical balance between three interfacial tension: solid–vapor (γ_{sv}), solid–liquid (γ_{sl}), and liquid–vapor (γ_{lv}). This mathematical representation of mechanical equilibrium is known as Young's equation:

$$\gamma_{lv}cos\theta_Y = \gamma_{sv} - \gamma_{sl} \tag{1}$$

θ represents Young's contact angle, and the relationship can be derived by means of simple mechanical equilibrium or energy balance.

Young's Eq. (1) contains only three measurable quantities [11], the contact angle θ, liquid–vapor surface tension, γ_{lv} and the solid surface energy γ_{sv} [12].

2.2. Surface energy and tension

Surface tension is caused by the cohesion between liquid molecules. In the interior of the liquid, the molecules are subject to uniform interactions in all directions. However, on the surface of the liquid, the forces around the molecules are not exactly the same, because there are gaps between the molecules. This disequilibrium results in a net inward force that pulls the molecules toward the interior of the liquid, resulting in a property called surface tension. The specific value of the surface

DOI: 10.54254/2755-2721/2025.29501

tension is affected by the type of interaction between liquid molecules. The measurement of surface tension has a wide range of applications in many industrial fields because it is directly related to the diffusion effect in coating formulations and is used in many other applications to evaluate the properties of surfactant solutions. As shown in the figure, this is a data table of the surface tension of a common liquid. Surface tension is measured in joules per square meter (J/m^2) or Newtons per meter (N/m), while the surface tension of liquids is usually in the range of 0.02 to 0.08 newtons per meter. In general, surface tension is expressed in mN/m or 10^{-3}N/m.

Substance	T	γ (mNm^{-1})	Substance	T	γ (mNm^{-1})
Water	10°C	74.23	Mercury	25°C	485.48
	25°C	71.99	Phenol	50°C	38.20
	50°C	67.94	Benzene	25°C	28.22
	75°C	63.57	Toluene	25°C	27.93
	100°C	58.91	Dichloromethane	25°C	27.20
Argon	90 K	11.90	*n*-pentane	25°C	15.49
Methanol	25°C	22.07	*n*-hexane	25°C	17.89
Ethanol	10°C	23.22	*n*-heptane	25°C	19.65
	25°C	21.97	*n*-octane	10°C	22.57
	50°C	19.89		25°C	21.14
1-propanol	25°C	23.32		50°C	18.77
1-butanol	25°C	24.93		75°C	16.39
2-butanol	25°C	22.54		100°C	14.01
Acetone	25°C	23.46	Formamide	25°C	57.03

Figure 4. Surface tension of common substances in different temperature. Yuki (2014) PPT - properties of liquids PowerPoint presentation, free download - ID:3016177, SlideServe. Available at: https://www.slideserve.com/yuki/properties-of-liquids (Accessed: 10 September 2024)

The energy associated with a surface, which we call surface energy, is the excess energy that goes with the surface. This energy is expressed as a quantity per square meter. It is crucial to recognise that surface energy can be described by two types of free energy: one is Gibbs free energy and the other is Helmholtz free energy. In addition, a clear distinction must be made between the surface energy GS and the surface tension γ, which are related but not identical concepts.

Measuring surface tension can be done by using a force tensiometer. The working principle of such devices is based on the determination of the force on the probe placed at the liquid-gas or liquid-liquid interface. The probe is connected to a highly sensitive balance and is in contact with the liquid interface under study. When the probe interacts with the surface of the liquid, the force recorded by the balance can be used to calculate the surface tension of the liquid. The strength of the measured force is affected by several factors, including the size and shape of the probe, the contact angle between the probe and the liquid, and the surface tension of the liquid. The size and shape of the probe are easy parameters to control. In order to ensure a zero-contact angle between the probe and the liquid being measured, the probe is usually made of platinum material. Two commonly used probe structures are Noüy ring and the Wilhelmy plate. In the case of a small sample volume, a metal rod can also be used to replace the Wilhelmy plate for measurement [13].

2.3. Wenzel vs. Cassie Baxter relation

The measurement of Young's contact angle is only suitable for smooth and uniform surfaces. For rough surfaces, Wenzel equation and Cassie-Baxter equation are needed to calculate the apparent contact angle of the liquid. The main difference between the Wenzel model and the Cassie-Baxter model is the difference in the contact area between the liquid and the solid surface. In the Wenzel model, the droplet is completely attached to a rough surface, while the Cassie-Baxter model

DOI: 10.54254/2755-2721/2025.29501

describes the droplet being present on both a solid surface and in air. In Wenzel state, if Young's contact angle exceeds 90 degrees, the liquid will show large apparent contact angle and significant contact angle hysteresis. Conversely, if the Young contact angle is less than 90 degrees, the liquid will exhibit a smaller apparent contact angle and a higher hysteresis. The figure below shows two different wetting states on a rough surface.

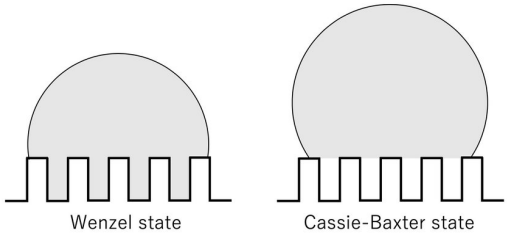

Figure 5. Illustration diagram of Wenzel and Cassie & Baxter equation. (No date) Wenzel State (left), Cassie-Baxter State (right). | download scientific diagram. Available at: https://www.researchgate.net/figure/Wenzel-state-left-Cassie-Baxter-state-right_fig1_257135729 (Accessed: 11 September 2024)

2.4. The principle of non-fluorinated hydrophobic materials

In general, creating a water-repellent surface mainly relies on two elements: low surface energy and high surface roughness. To prepare surfaces with these properties, there are two main technology paths: a top-down approach that covers plasma processing, lithography, and template-based techniques; The other is a bottom-up approach, including chemical deposition, layer-to-layer (LBL) deposition, hydrogen bonding, sol-gel process, and colloidal assembly techniques. In the field of bottom-up technology, methods such as coating the surface with paraffin wax, treating the fiber surface with pyridine compounds, silicone resins or fluorocarbons have been widely used to achieve the waterproof effect of fabric surfaces [14].

3. Natural superhydrophobic surfaces and stain-resistant surfaces

Since ancient times, people have learned a lot from nature, and research on imitating and learning from these creatures has brought great improvements to human life. Nowadays, people are still striving to learn more from nature. In the research of water repellent materials, we have noticed that many creatures in nature possess such characteristics, which help them stay clean and even survive in challenging environments. For example, lotus leaves, Salvinia, and water-repellent creatures have unique mechanisms that we can draw inspiration from. By studying and imitating these natural phenomena, researchers aim to develop a new generation on non-fluorinated DWR coatings and materials.

3.1. Natural water repellent

3.1.1. Lotus leaves

The lotus leaves are renowned for their unique self-cleaning ability. This ability exists on the surface of the lotus and allows any adherent dust particles to be removed by raindrops [15]. As is shown in Fig.5 and 6, the leaf is covered with tiny papillae structures, which are spaced apart in such a way that they trap air, creating an extremely thin air film. When water droplets land on the lotus leaf, due

DOI: 10.54254/2755-2721/2025.29501

to this special micro-nanostructure, the water is unable to penetrate the leaf's surface. Instead, it rolls off readily, thereby keeping the leaf dry and clean. This natural superhydrophobicity of the lotus leaves not only prevents water retention but also reduces the adhesion of dirt and microorganisms, making it a clever self-preservation mechanism in nature.

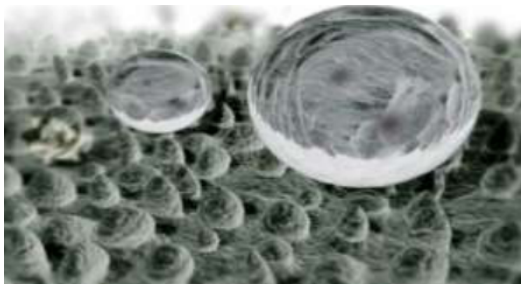

Figure 6. Spherical water drop on surface of lotus leaf hierarchical structures [16]

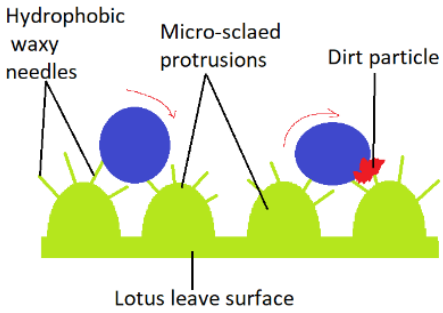

Figure 7. Dirt particles removed by raindrops from the Lotus leaves' surface [15]

3.1.2. Salvinia

Salvinia is also renowned for its remarkable hydrophobic properties. The leaf has the ability to retain rain for long periods when submerged in water [17]. This remarkable feature is attributed to the unique microstructure of its leaves, specifically the densely packed hairs covering their surface. As is shown in Fig.7, these microscopic hairs, known as trichomes, create a physical barrier that traps air beneath the leaf surface, forming a thin layer of air cushions. This air-water interface significantly reduces the contact area between the water and the leaf, resulting in a strong hydrophobic effect [18]. When water comes into contact with the leaf, it encounters minimal surface contact due to the air cushions, causing the water droplets to bead up and easily roll off.

This natural hydrophobicity not only aids in the plant's buoyancy and survival in aquatic environments but also inspires biomimetic designs in various fields, such as the development of self-cleaning surfaces, and water-resistant materials.

DOI: 10.54254/2755-2721/2025.29501

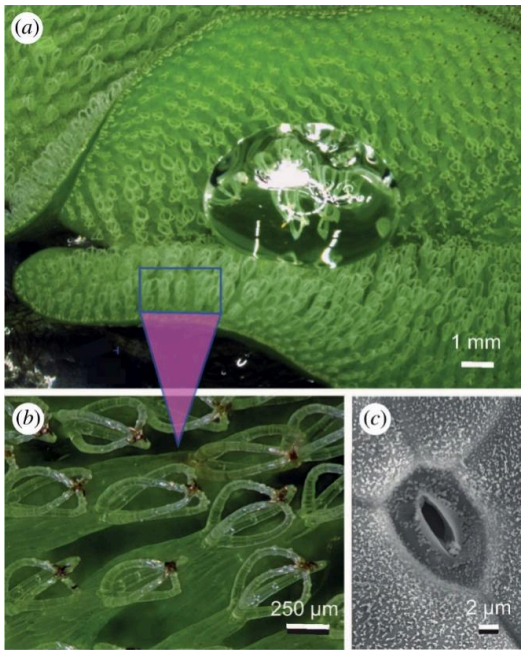

Figure 8. (a) Salvinia molesta's leave, showing the highly hydrophobic 'egg beater' trichomes. (b) A close-up view of the egg-beater trichomes. Egg-beaters are supported by a columnar structure called an 'emergence'. (c) Stoma at the base of the upper surface of the leaf. Note the whitish texture of wax crystals covering the entire leaf surface [17]

3.1.3. Water strider

The water strider is a fascinating insect that exhibits remarkable hydrophobic properties. These properties allow the water strider to effortlessly traverse the surface of water without sinking or wetting its body. This feature was believed to be due to the repellency caused by a secreted wax [19]. As is shown in Fig.8, in reality, however, the superhydrophobicity of the water strider's legs is related to the particular hierarchical structure of the legs, which are covered by many oriented tiny hairs with fine nanogrooves [20].

As the water strider moves across the water's surface, its legs act like paddles, pushing against the thin film of water without actually penetrating it. The trapped air bubbles provide buoyancy, allowing the insect to glide effortlessly on the water's surface.

The hydrophobicity of the water strider's legs not only enables its unique mode of movement but also inspires scientists and engineers to develop new materials and technologies with similar properties.

DOI: 10.54254/2755-2721/2025.29501

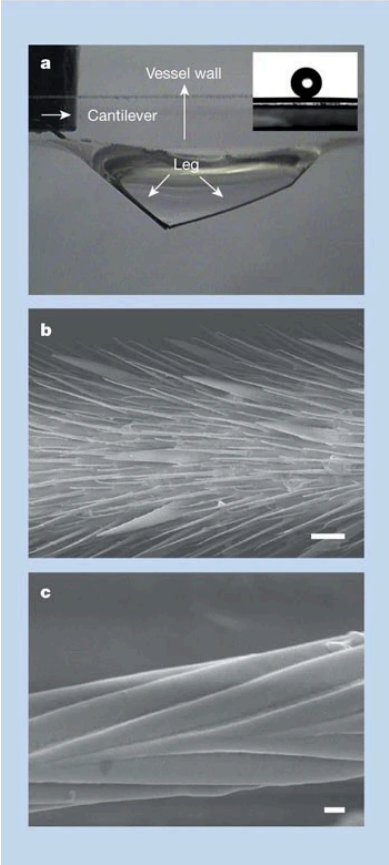

Figure 9. a, Typical side view of a dimple at its maximum depth (4.38 ± 0.02 mm) before the leg penetrates the surface of the water. The contact angle is 167.6 ± 4.4°. b, c, Scanning electron micrographs of a limb showing numerous oriented spiky microsetae b and the delicate nanoscale ripple structures on a (C). Scale bars: b, 20 μm; c, 200 nm [20]

3.1.4. Springtails

Springtails exhibit remarkable hydrophobic properties. These properties allow them to thrive in a wide range of environments, including those with high humidity or even temporary waterlogging. As is shown in Fig.9, the key to their hydrophobicity lies in their unique body structure, particularly their exoskeleton, which is covered with a layer of waxy or oily substances. This layer acts as a barrier, preventing water from easily penetrating the insect's body [21]. The re-entrant texture present on the skin of some springtails enable them to repel not just water, but also a wide range of low surface tension liquids such as various oils and alcohols.

DOI: 10.54254/2755-2721/2025.29501

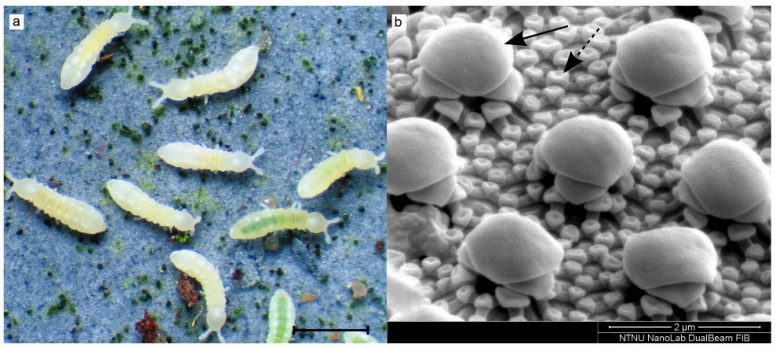

Figure 10. Live Collembola and their cuticle structure (a) Multiple samples of Onychiurus sp., scale bar 1 mm. (b) It shows a pattern of large secondary granules (solid arrows), interspersed with a pattern of small primary granules (dashed arrows), which are joined together with ribs [22]

3.2. Natural stain-resistant surfaces

Many materials draw inspiration from nature. In fact, our research on stain-resistant materials was inspired by it [23]. The biological structures mentioned above are crucial for the formation of hydrophobic surfaces. Plants and organisms such as lotus, butterflies, and water strider exemplify natural resistance to pollution in nature through their unique texture and chemistry. These organisms not only maintain cleanliness and elegance in a polluted environment but also provide valuable inspiration for humanity. For instance, we can leverage the lotus leaf effect to develop self-cleaning materials for clothing, construction, and other industries. Likewise, we can draw insights from the leg structure of water striders to engineer a robot capable of walking or gliding on water. These applications not only help reduce pollution and protect the environment but also drive scientific and technological progress.

4. Synthetic Surfaces

Non-fluorinated superhydrophobic fabrics/ Stain-resistant fabrics:

4.1. Preparation methods

We briefly discuss the principles of four kinds of preparation techniques used to create non-fluorinated, durable water repellent synthetic surfaces in the following section.

4.1.1. Etching and lithography

In general, we can divide etching technique into four categories, including conventional wet etching, conventional dry etching, photoelectrochemical (PEC) etching and metal-assisted chemical etching (MacEtch). The main differences between these four methods are the etch rate, orientation dependence and control, etching mechanism, surface quality, and proposed reaction.

Wet etching uses chemical solutions to selectively remove material from a substrate, creating a textured surface. This process is guided by the principle of differential etch rates, where certain crystal planes of the material etch faster than others. For instance, in the case of silicon, anisotropic etching, a common technique that can be used in wet etching, dry etching, and so on, can result in the formation of pyramidal or inverted pyramidal structures, which are crucial for water repellency. The simplicity and cost-effectiveness of wet etching make it a popular choice for initial prototyping.

DOI: 10.54254/2755-2721/2025.29501

However, it may lack the precision required for intricate patterns, limiting its application in high-resolution surface fabrication.

Dry etching is commonly compared to wet etching, as both are traditional etching techniques. The most notable difference between these two methods is the etchant they utilize. The etchant used in dry etching is in the vapor phase, while wet etching employs a plasma to remove material from the substrate, providing greater control and precision. Techniques like reactive ion etching (RIE) and deep reactive ion etching (DRIE) are capable of producing high-aspect ratio features and complex 3D structures. The use of ion beams in ion beam etching (IBE) allows for the creation of ultra-fine patterns, which are essential for advanced water-repellent surfaces. Dry etching's ability to maintain structural integrity during the removal process makes it ideal for applications requiring nanoscale precision. In this way, it's popular in the field of modern device fabrication, due to its better controllability and anisotropy [25].

Photolithography is a cornerstone of modern silicon chip fabrication, utilizing light to transfer patterns onto a substrate. The process begins with the application of a photoresist, a light-sensitive material that hardens upon exposure to light. By projecting a pattern through a photomask onto the resist, the desired pattern is imprinted. Etching steps then reveal the pattern on the silicon substrate. Photolithography's universability and scalability have made it to become a standard in the semiconductor industry, and its precision is invaluable for creating water-repellent surfaces with controlled microstructures. However, it is not without its drawbacks, such as the potential limitations in manufacturing high-resolution patterns due to light wavelength constraints, scaling beyond the size of a typical silicon wafer, and photoresist edge roughness.

Fig. 10. shows a SEM image of a Ga_2O_3 surface treated with plasma enhanced chemical etching (PEC etching) to illustrate the process. In the figure, it is clear that white flaky dendritic particles are formed on the surface of Ga_2O_3. The appearance of these particles indicates the presence of gallium salt, which plays a key role in the process of etching Ga_2O_3 by PEC. The structure of these dendritic particles is similar to the morphology observed during chemical mechanical polishing (CMP), which indicates that selective and non-uniform chemical reactions occur on the surface of Ga_2O_3. The relative cleanliness of the gallium salt surface compared to the gold mask, although the gallium salt is difficult to remove from the surface, suggests that dissolution and redeposition are very likely to be present in the process, highlighting the complex dynamics involved in the etching process.

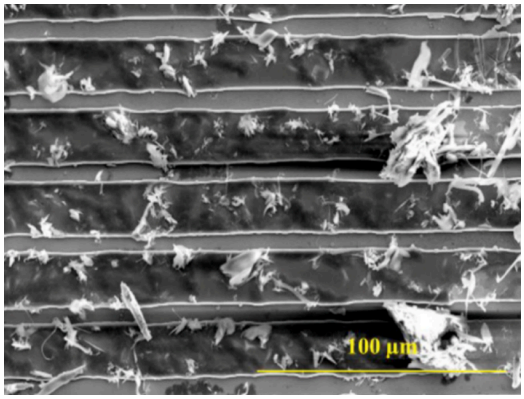

Figure 11. SEM image of Ga_2O_3 after PEC [26]

Metal-assisted chemical etching (MacEtch) is a unique electrochemical technique for fabricating high-aspect-ratio nanostructures with smooth sidewalls and minimal plasma-induced damage. This process utilizes a noble metal catalyst, such as gold or platinum, to drive the selective removal of

DOI: 10.54254/2755-2721/2025.29501

semiconductor material. MacEtch excels in creating structures with aspect ratios exceeding 100:1, making it ideal for applications requiring deep and narrow features, such as microfluidic chips and photonic crystals. Unlike traditional etching, MacEtch produces smooth and vertical sidewalls, reducing scattering losses and improving device performance. Its plasma-free nature eliminates the risk of ion-induced damage, further enhancing device reliability. While MacEtch faces challenges like orientation dependence and slower etch rates, ongoing research aims to develop new catalyst materials and optimize etching conditions for broader applications [24].

Phan et al, reported research that employed MacEtch combined with surface modification to fabricate nanomaterials with enhanced hydrophobicity and self-cleaning properties. The process started with the self-assembly of a monolayer of silica particles on a silicon wafer. Then after argon ion bombardment, the particle size decreases. As the silicon dioxide particles are then used as a mask, gold is deposited onto the wafer to form a gold layer with regularly spaced openings. Subsequently, the wafers were subjected to MACE using a mixture of hydrofluoric acid and hydrogen peroxide to selectively etch the silicon exposed through the gold mask, leaving behind arrays of high aspect ratio silicon nanowires.

To enhance the hydrophobicity of the silicon nanowires, an octadecyltrichlorosilane (OTS) layer was deposited on the surface. Since OTS has low surface energy hydrophobic end groups and siloxane bonds, it can be immobilised on the silicon surface, after which the free energy of the surface is reduced, increasing the repulsion of water droplets. The high-aspect-ratio nanowire structure further contributes to hydrophobicity by increasing the surface area in contact with the droplet, resulting in a high contact angle and low sliding angle.

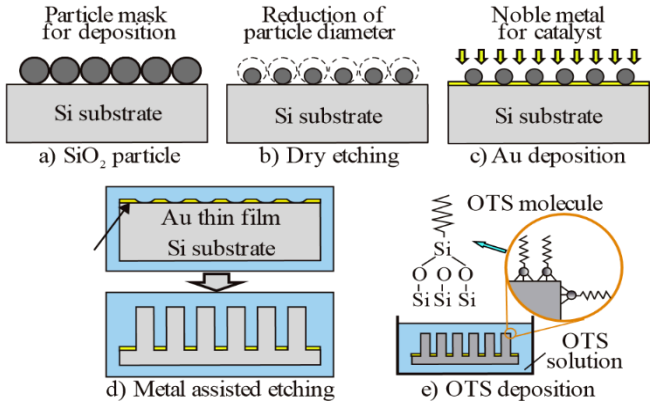

Figure 12. Fabrication process: (a) SiO_2 hydrophilic layer is formed on the silicon substrate (b) Reducing the diameter of the SiO2 particles through dry etching (c) Deposition of a precious metal catalyst layer on the silicon (d) Etching of silicon using the metal catalyst layer to create nanostructures (e) Deposition of OTS molecules on the nanostructured silicon surface for functionalization

DOI: 10.54254/2755-2721/2025.29501

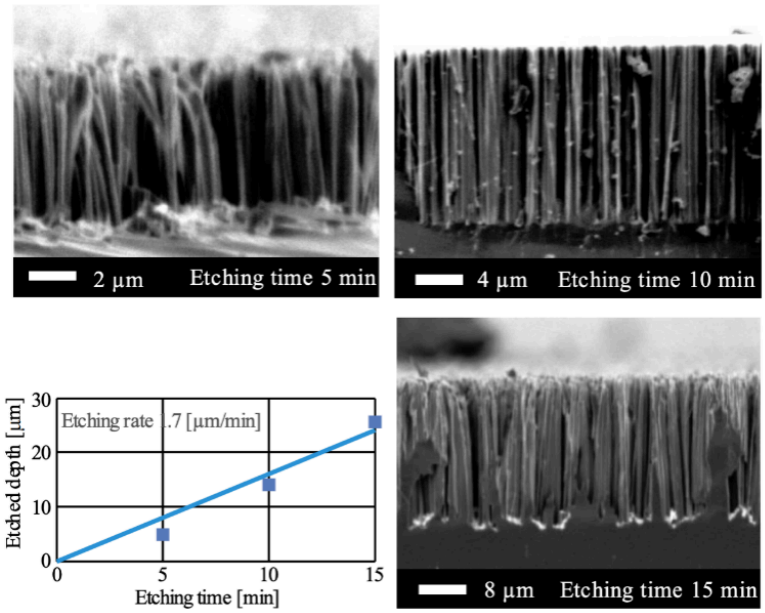

Figure 13. The structures caused by different etching times and the relationship between etching depth and time

The combined effect of the OTS layer and the high-aspect-ratio nanowires yielded a surface with a contact angle exceeding 150° and a sliding angle of less than 1°, demonstrating excellent self-cleaning properties (as shown in Fig. 13.). This material holds potential for applications in microfluidic chips, sensors, and other fields. However, it is worth noting that the current MACE structure is not completely oleophobic due to the assumption that it lacks a re-entrant texture and therefore does not repel some low surface energy liquids (e.g., oils) very well. Future research efforts should focus on developing strategies to enhance the omniphobicity of MACE structures [27].

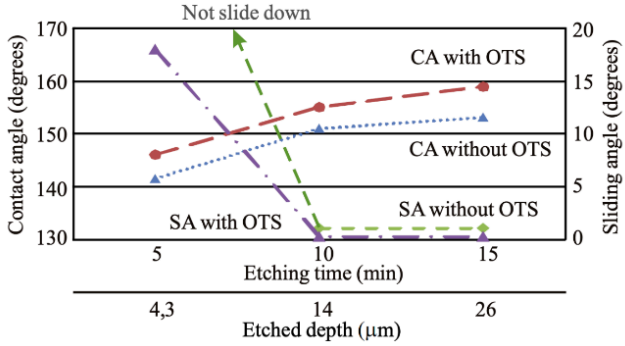

Figure 14. The relationship between CA, SA, and etching time and depth

4.1.2. Layer-by-Layer (LBL) assembly method

Layer-by-Layer (LBL) assembly method is a kind of technology that is able to prepare certain materials by sequentially depositing polyelectrolytes, nanoparticles, or polymer brushes onto the surface of a substrate material. By controlling parameters such as solution concentration, ionic strength, pH, and van der Waals force, we can precisely regulate the thickness, composition, and structure of the resultant films, thereby fine-tuning the surface properties [28].

DOI: 10.54254/2755-2721/2025.29501

Ye et al. reported relevant research in this regard. First, chitosan (CS) and lignosulfonate (LGS) were dissolved in solutions to prepare solutions with a concentration of 2 mg/mL. Subsequently, a single crystal silicon wafer was used as the substrate and cleaned using piranha solution and $H_2O/H_2O_2/NH_4OH$ solution to remove surface impurities. Finally, by controlling the dipping process, LGS and CS solutions were alternately coated on the substrate, forming multilayer films through electrostatic attraction. By altering the coating sequence and controlling the van der Waals forces, CS and LGS films with different surface morphologies and hydrophobicity could be prepared.

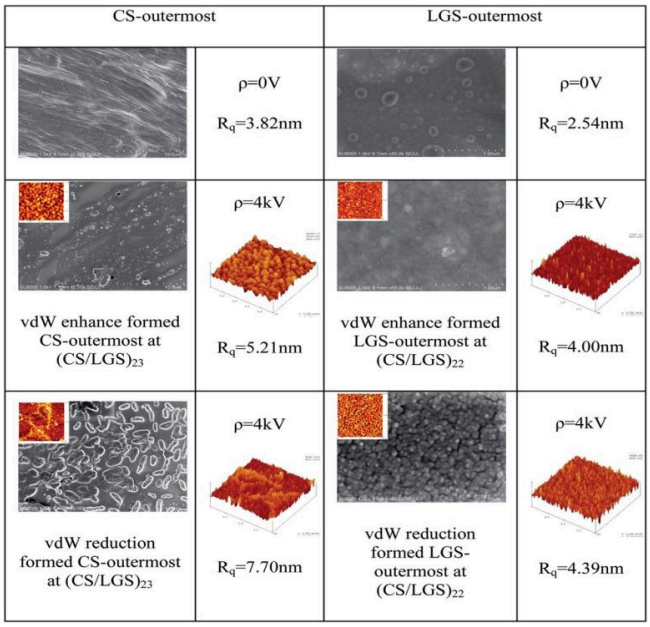

Figure 15. Images of FESEM and AFM of CS outer layer and LGS outer layer $(CS/LGS)_n$ multilayered nanofilms and the relation between changes in their wetting capacity and changes in van der Waals' forces with

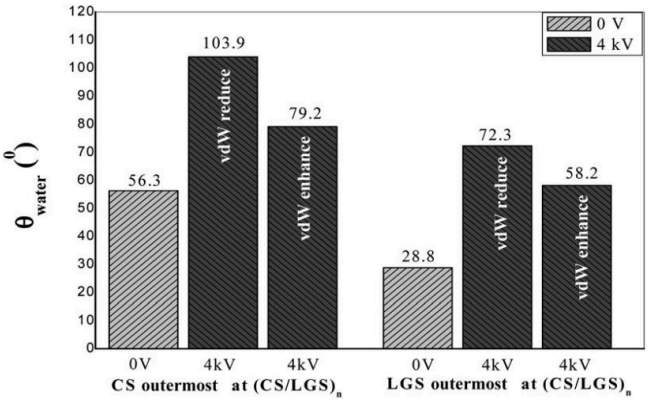

Figure 16. The wettability of CS and LGS surfaces formed by the LBL electroassembly method was associated with enhanced or reduced van der Waals attraction at 0 V or 4 kV [29]

As shown in Fig. 14.15, it is illustrated that the CS/LGS films prepared by the van der Waals force reduction process have a higher surface roughness and a larger contact angle compared to other methods, which suggests that the films are hydrophobic. This finding aligns with previously reported literature. The results of the analyses further indicate that in the LBL electroassembly

DOI: 10.54254/2755-2721/2025.29501

technique, the surface tension of the polymer solution decreases due to the intervention of the electrostatic field, a change that directly affects the formation of the final film and its configuration. In addition, the LBL electroassembly technique allows a bidirectional regulation of van der Waals forces - both enhanced and weakened - a property that significantly determines the microstructure of the film surface and the degree of its hydrophobicity.

4.1.3. Electrochemical reaction and deposition

Electrochemical reactions consist of two main methods. Electrochemical anodization and micro-arc oxidation coatings are two common techniques used to create certain surface coatings.

Electrochemical anodization uses ions from an electrolyte solution to form an oxide coating on the surface of a metal substrate. The process commonly involves applying a voltage between a cathode and an anode, with the metal substrate as an anode to accept electrons, resulting in the formation of an oxide layer. This oxide layer usually has a porous structure which can enhance the adhesion and chemical stability of the coating. Generally, electrochemical anodization coatings are widely used in the aerospace, automotive and construction industries to enhance the corrosion, hardness and wear resistance of materials.

Micro-arc oxidation happens when the voltage exceeds a certain threshold during the anodization process, resulting in the formation of tiny arc discharges on the coating surface. Also, these discharge points generate high temperatures, leading to partial melting and ablation of the coating surface and resulting in the formation of a dense oxide layer. Micro-arc oxidation coatings offer higher hardness and wear resistance, making them fit for applications requiring greater durability, such as cutting tools, molds and wear parts.

Both methods involve an electrochemical process, but micro-arc oxidation is distinguished by its unique discharge process, which creates a denser and more durable coating. When choosing between these two methods, it is essential to consider the specific requirements of the application and the desired properties. For example, if high corrosion resistance is required, electrochemical anodic oxidation may be the preferred method. On the contrary, if the coating needs to be harder and more wear resistant, microarc oxidation may be more appropriate [30].

Electrochemical deposition (ECD) technology has become a common method of preparing superhydrophobic surfaces due to its simplicity, controllability, cost effectiveness and the ease with which large areas can be modified. By electrostatically depositing ions or charged nanoparticles onto a conductive substrate, ECD technology can form micro/nanostructures that impart superhydrophobic properties to the surface. ECD technology can be applied not only to metallic surfaces, but also to non-metallic and composite surfaces, enabling the manufacture of superhydrophobic coatings with excellent properties. In the future, we believe that the ECD technology will continue to evolve towards increased stability, environmental friendliness, and multifunctionality, paving the way for the wider application of superhydrophobic coatings in various fields.

Jain et al. published a report that copper-based superhydrophobic coatings were fabricated using a two-step electrodeposition process and modified with stearic acid for enhanced hydrophobicity. Cleaned copper sheets served as the working electrode, with platinum as the counter electrode and another copper sheet as the reference electrode. The deposition was conducted in an aqueous solution containing copper sulfate and sulfuric acid, applying overpotentials ranging from 0.5 V to 1.1 V for 30 minutes. A subsequent deposition step at 0.15 V for 10 seconds was employed to stabilize the morphology. The coated samples were then immersed in a 0.02 M stearic acid methanol solution for 24 hours, followed by washing with water and drying.

DOI: 10.54254/2755-2721/2025.29501

Scanning electron microscopy revealed that increasing the overpotential led to a transition from needle-like structures to spherical features, ultimately forming a multiscale, fractal, cauliflower-like morphology. As shown in Fig. 16, This unique structure effectively trapped air, resulting in a stable Cassie state and exceptional hydrophobicity with contact angles exceeding 160°. The coatings also exhibited a low contact angle hysteresis, indicating good dynamic wettability.

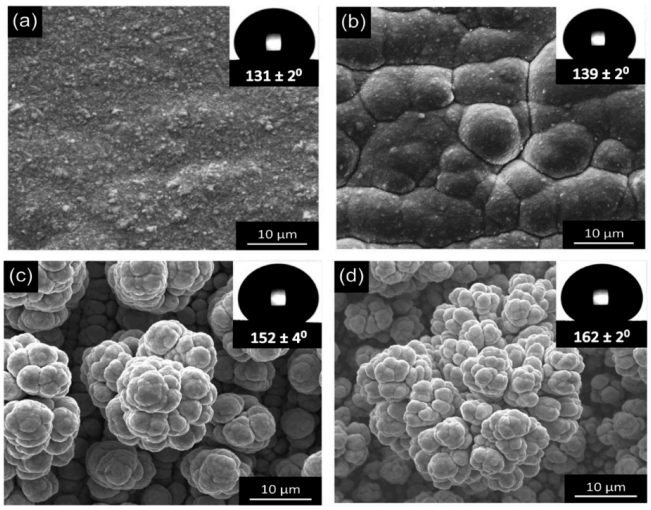

Figure 17. SEM images and corresponding water droplet contact angles for copper samples prepared at varying applied overpotentials: (a) 0.5 V, (b) 0.7 V, (c) 0.9 V, and (d) 1.1 V, illustrating the development of spherical protrusions beyond an overpotential of 0.7 V [31]

4.1.4. Colloidal templating

Colloidal templating is a fabrication method for superhydrophobic surfaces that combines self-assembly with photolithography. It utilizes pre-prepared colloidal crystals as templates to aggregate colloidal particles by removing solvents, and forming surfaces with specific shapes, sizes, and structures. This surface then guides the next coating material to self-assemble, resulting in superhydrophobic coatings with the desired morphology. This method offers a high degree of controllability and allows the preparation of superhydrophobic coatings with different coating morphologies and functionalities such as anti-fogging, anti-fouling and self-cleaning. However, this method also has some restrictions, such as the difficulty in the preparation of colloidal templates of precise shape and size, the difficulty in controlling the self-assembly process and the need to select appropriate template disposal methods to avoid damage to the coating. Despite these limitations, the prospects for the use of colloidal templating in the manufacture of superhydrophobic surfaces could be greatly expanded with further development of the technology [32,33].

Kong et al. reported a related experiment in which they successfully used the colloidal template method to prepare a hydrophobic porous Au-Ag alloy nanoparticle array. Kong et al. reported a related experiment in which they successfully used the colloidal template method to prepare a hydrophobic porous Au-Ag alloy nanoparticle array.

Using a gas-liquid interfacial self-assembly technique, the researchers successfully constructed a monolayer crystal lattice of polystyrene (PS) colloidal particles with a 500-nm periodic structure on a quartz substrate. They then applied an Au film to this crystal array in just one minute by sputtering. The samples were annealed at different temperatures (200 °C-1000 °C, the interval is every 200 °C) for 2.5 hours at each temperature point to form an array of Au nanoparticles. The annealing process

DOI: 10.54254/2755-2721/2025.29501

was finally selected at 1000°C, because at this temperature, the Au nanoparticles formed showed an orderly and regular arrangement without obvious and fine Au nanoparticles.

Subsequently, they covered the surface of the arrays with a layer of silver (Ag) film and successfully prepared well-arranged Au-Ag alloy nanoparticle arrays by heat treating them for two hours under a mixed atmosphere of N_2 and H_2. In the final stage of the process, they immersed the arrays in a 50% HNO_3 solution for etching. By adjusting the deposition duration of the Ag film, it was possible to precisely manipulate the pore size.

In order to form a surface with hydrophobic properties, a gold film also needs to be deposited on the surface of the array just prepared. By observing the obvious change in the contact angle of the surface, it can be found that this layer of gold film obviously changes the surface property from hydrophilic to hydrophobic. It is speculated that the complex nanoscale structure formed after Au film deposition, which greatly reduces the surface roughness and surface energy of the array surface, resulting in the above changes.

SEM images reveal the relationship between pore size of template and hydrophobicity. It was observed that the hydrophobicity of the prepared nanoparticle arrays first increased and then decreased with the increase of the colloidal template pore size. When the colloidal template pore size is smaller, the surface roughness of the nanoparticle array is higher, which leads to a more complex nanoscale structure, which reduces the surface energy, enhances the hydrophobic effect, and thus increases the contact Angle, showing better hydrophobic properties.

By contrast, when the pore size of the colloidal template was too large, leading to an increase in surface energy and weakened hydrophobicity, because the surface roughness of the nanoparticle arrays decreased and the nanostructured hierarchical structure disappeared, as a result, the contact angle decreased and the hydrophobicity decreased.

As shown in Fig.17 and Table. 2, The results show that the pore size of the colloidal template is a key factor influencing the hydrophobicity of the nanoparticle arrays. By controlling the pore size of the colloidal template, nanoparticle arrays with different hydrophobic properties can be prepared to meet various application requirements.

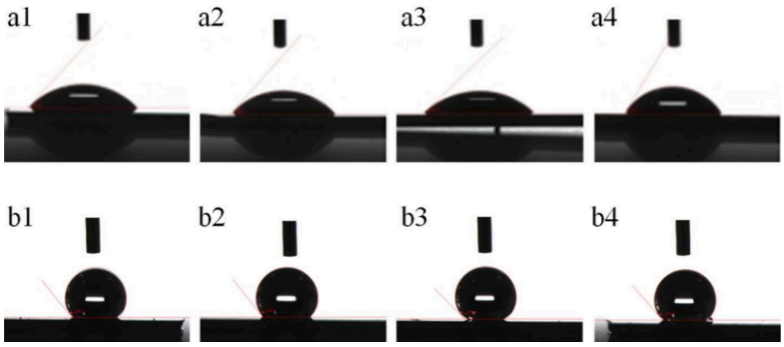

Figure 18. The surface wettability of porous Au-Ag alloy nanoparticle arrays in various silver film deposition times: 60 s (a1 and b1), 90 s (a2 and b2), 120 s (a3 and b3), and 150 s (a4 and b4). Among them, groups a1 to a4 are the states before gold film deposition, and groups b1 to b4 are the states after gold film deposition

DOI: 10.54254/2755-2721/2025.29501

Table 2. Contact angle variation of gold-silver alloy nanoparticle arrays before and after gold film deposition [34]

Sample	CA			
Before depositing	47.51	48.06	43.80	58.71
After depositing	129.18	128.77	135.03	131.59

4.2. Materials utilized for fabricating DWR coatings

4.2.1. Silicones

Polydimethylsiloxane (PDMS) is a widely used as hydrophobic material today because of its extremely low surface energy. In addition, PDMS also has several remarkable advantages, like flexibility, biocompatibility, good chemical stability, strong non-adhesive properties and ease of processing. In order to give full display to the advantages of PDMS, more and more researchers have devoted themselves to the development of PDMS research in recent years. Therefore, direct and indirect methods have been developed to fabricate superhydrophobic PDMS surfaces [35].

In the direct method, the PDMS surface is directly modified, such as via the introduction of nanostructures on the surface of the PDMS. Sun et al. reported a one-step method for the convenient and rapid fabrication of superhydrophobic and photothermally active PDMS elastomeric materials for light-driven floating devices. First, a PDMS film is prepared by mixing the PDMS prepolymer with a curing agent and curing it. Then, a CO_2 laser engraving machine is used for laser processing. Laser cutting mode is employed to cut the PDMS film into various shapes, while laser engraving mode is used for surface modification of the PDMS devices, making the surface rough and causing carbonization, thereby imparting superhydrophobicity and photothermal activity to the material. The material produced by this method exhibited a WCA of 153 degrees, demonstrating superhydrophobicity [36].

In the indirect method, templated replication is an effective approach to fabricate flexible superhydrophobic PDMS surfaces. It utilizes laser processing or chemical etching techniques to create templates with specific microstructures, and then casts PDMS onto these templates for curing, ultimately yielding flexible PDMS films with superhydrophobic properties.

Wu et al. report a method of fabricating flexible superhydrophobic PDMS surfaces. As shown in Fig. 18, in this research, researchers used two methods to prepare templates and ultimately obtained four different surface morphologies of PDMS films, named S1, S2, S3, and S4.

S1: Prepared by etching with hydrochloric acid. The PDMS film has a random rough "wind-erosion topography" structure, similar to the natural landforms formed by wind erosion, with irregular concave and convex shapes.

S2: Prepared by laser etching at 90°. The PDMS film has a regular protruding structure, with these protrusions arranged linearly, forming an orderly microstructure.

S3: Prepared by laser etching at 0°. The PDMS film has a regular protruding structure, with these protrusions arranged in concentric circles, forming an orderly microstructure.

S4: Prepared by laser etching simultaneously at 0° and 90°. The PDMS film has a more complex regular protruding structure, with these protrusions interlacing, forming a more three-dimensional microstructure.

S5: Unprocessed PDMS film.

DOI: 10.54254/2755-2721/2025.29501

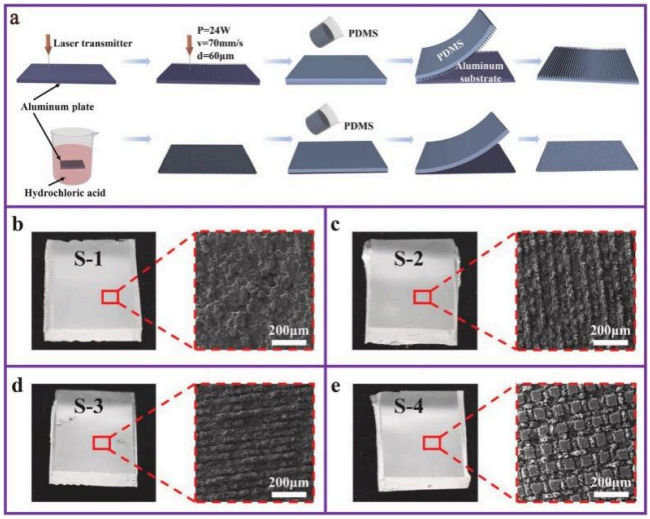

Figure 19. (a) Process for preparing PDMS superhydrophobic surface. And the modification of the microstructure on the surface includes: (b) treatment of the aluminum substrate with hydrophobic acid etching technology, (c) 90° laser etching of the substrate, (d) 0° laser etching of the substrate, and (e) simultaneous 0° and 90° laser composite etching of the substrate

The static contact angle and rolling angle of different films were measured, and their self-cleaning performance was observed.

The experimental results show that all PDMS films (S1, S2, S3, and S4) prepared by template replication exhibit excellent superhydrophobicity, with a contact angle of about 150° and a rolling angle of less than 5°. This means that water droplets are difficult to adhere on these surfaces and can easily roll or slide off, thus achieving a self-cleaning effect.

As shown in Fig. 19, experiments observed that when water droplets roll on superhydrophobic surfaces, they can easily take away surface pollutants, restoring them to a clean state. For example, after cleaning with water, the PDMS film contaminated with fine sand quickly returns to its original superhydrophobic state, and water droplets can still easily roll off. This indicates that superhydrophobic surfaces have good self-cleaning performance, which can effectively prevent the adhesion and accumulation of pollutants. As shown in Fig. 2a, S1-S4 still maintain superhydrophobicity after cleaning, while S5 is still covered with sand.



Figure 20. The self-cleaning ability of the prepared superhydrophobic PDMS surface (S1-S4) and the planar flexible PDMS surface (S5), as well as the water contact Angle and surface roughness changes before and after the self-cleaning process [37]

DOI: 10.54254/2755-2721/2025.29501

4.2.2. Organic materials

Based on existing research data, most polymers exhibit hydrophobicity, with polyethylene (PE) alone accounting for 30% of the market share. Considering its economic viability and easy accessibility, prior work has investigated the application of PE as a superhydrophobic surface [38].

Pinheiro et al. published a report stating that vertically aligned carbon nanotubes (VACNT) inherently possess superhydrophobicity. Therefore, their experimental approach involved comparing the contact angle changes between VACNT with and without PE growth to explore the hydrophobic effects of PE. They first grew VACNT on stainless steel substrates using thermal chemical vapor deposition (TACVD). Subsequently, they subjected some VACNT samples to CO_2 laser treatment to form a cage-like structure, enhancing the surfaces superhydrophobicity. Finally, they dipped the VACNT samples into xylene containing PE to coat them with PE. Additional control experiments were conducted, such as plasma oxidation of some VACNT samples to convert them into superhydrophilic surfaces for comparison. The contact angles of these mentioned samples are shown in Table.3.

Table 3. The contact angles of the various materials prepared [39]

Sample format	Description	Formats	CA (°)
BARE	Sainless-steel surface without further treatment	Tube and square	87±1
BARE-PE	Sainless-steel surface with PE deposition	Tube and square	106±2
VACNT	Sainless-steel with as grown VACNT	CA	153±1
VACNT-PE	VACNT sample with PE deposition	Tube and squere	169±2
VACNT/laser	VACNT sample submitted to laser treatment	CA	160±2
VACNT/laser-PE	VACNT/laser sample with PE deposition	Tube and square	160±2
VACNT/ox	VACNT sample oxidized by plasma	Tube	<2
VACNT/ox-PE	VACNT-ox with PE deposition	CA	156±2

The results showed that the PE coating played an important role in enhancing the hydrophobicity of the VACNT surface. The PE coating effectively increased the superhydrophobicity of the VACNT surface, which resulted in an increase in the contact angle. This was due to the polyethylene coating lowering the surface energy of VACNT, making it more likely for water droplets to form and reducing the adhesion of water droplets to the surface. It was also found that CO_2 laser treatment further enhanced the superhydrophobicity of VACNT and led to the formation of a unique cage-like structure on the surface.

4.2.3. Inorganic materials

Currently, the fabrication of purely inorganic superhydrophobic materials usually requires the treatment of Zn by electrodeposition to obtain a rough Zn coating. The coatings are then modified with materials having low surface energy, and ZnO nanomaterials are a suitable choice for this purpose due to their diverse morphology and relatively low cost [40].

Li et al. published an experimental report on the fabrication of ultra-waterproof Zn/ZnO coatings with excellent water resistance and anti-corrosion properties. In this study, a two-step electrodeposition method and subsequent chemical treatment were used to successfully fabricate ultra-water-resistant, pine-needle morphology Zn/ZnO coatings (Zn/ZnO-3) on the surface of carbon steel. Initially, a homogeneous and compact multi-faceted micron-sized zinc layer was formed on a

DOI: 10.54254/2755-2721/2025.29501

carbon steel substrate by electrodeposition. Immediately after, in a second stage of electrodeposition, on top of the polyhedral zinc layer, radially ordered ZnO nanorods were deposited, forming a pine-needle structure. Finally, the coating was immersed in a stearic acid ethanol solution to reduce the surface free energy and achieve superhydrophobicity, as shown in Fig. 21.

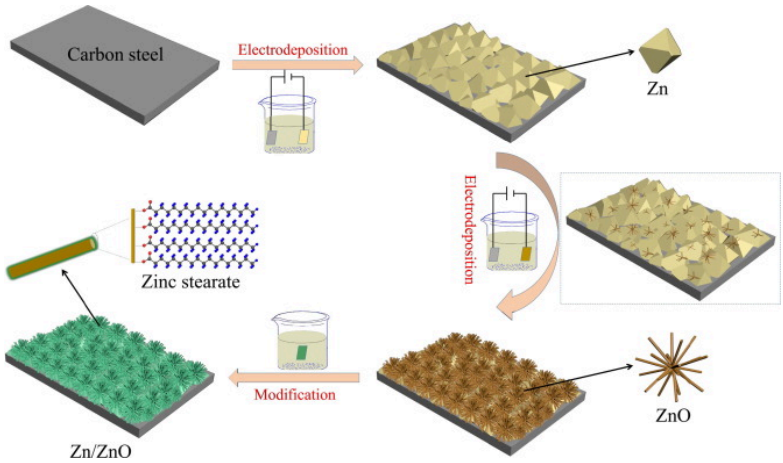

Figure 21. The process of fabricating hierarchical structured Zn/ZnO by electrodeposition

As shown in Fig. 22, the surface morphology and composition of the coating were characterized in detail by scanning electron microscopy (SEM). SEM images clearly reveal the gradual change of coating morphology. During the initial electrodeposition phase, a uniform and dense micron-sized zinc polyhedral layer was successfully accumulated on the carbon steel surface. In subsequent electrodeposition steps, ZnO nanorods started to emerge and constructed a radial arrangement on top of the newly coated Zn layer. With increasing deposition time (corresponding to Zn/ZnO-1,2,3, from short to long), the size and number of ZnO nanorods progressively increase until they fully cover the faceted Zn layer, shaping a unique pine-needle-like surface structure.

DOI: 10.54254/2755-2721/2025.29501

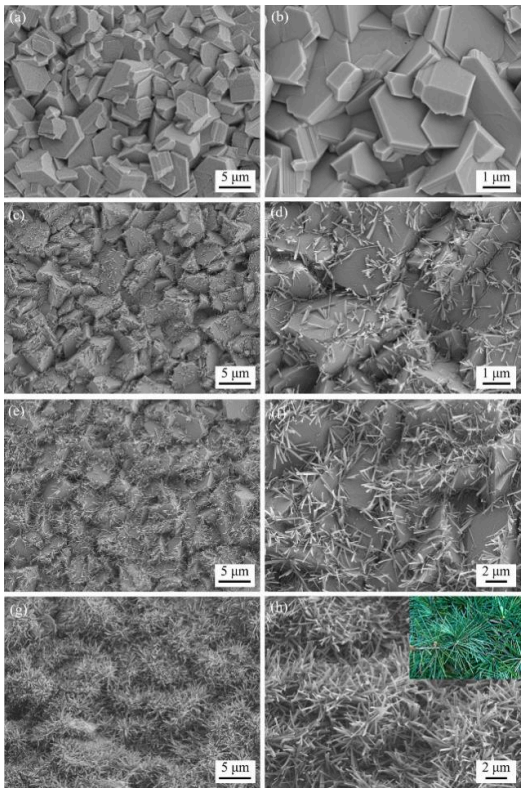

Figure 22. SEM images of Zn/ZnO series coatings, including Zn (a-b), Zn/ZnO-1 (c-d), Zn/ZnO-2 (e-f) and Zn/ZnO-3 (g-h)

The wettability of the coating was evaluated by the WCA and SA. The results showed that with the continuous growth of ZnO nanorods, the water contact Angle of the acicular Zn/ZnO coating gradually increases until it reaches a high value of 166.8±1.4°, while the sliding Angle remains at a very low value of 2.6±0.5°, showing excellent superhydrophobic properties. In addition, the coating is highly repellent to a variety of liquids, like milk, tea, methylene blue and so on, and the surface contact Angle with these liquids is more than 155.3° [41].

4.3. Stain resisting via non-fluorinated material

Stain-resisting properties are somewhat related to hydrophobicity, as both are achieved by reducing the surface free energy of materials. If the surface free energy of a material is low, it will have excellent resistance to solid and liquid particle contamination. Just as the lotus leaf in nature has relatively low surface free energy, it has notable hydrophobicity and stain-resisting properties.

This principle has also been adopted by industry for imparting anti-pollution properties to materials, such as surface modification of stainless steel which is used in a number of industries due to its excellent anti-corrosion properties. However, its surface is prone to contamination and corrosion, which limits its application range. To address this issue, people have tried to transform the surface of stainless steel into a superhydrophobic surface to achieve the purpose of stain resistance and anti-corrosion. Traditional methods for preparing superhydrophobic surfaces usually require the use of fluorine-containing materials for low surface energy modification.

Xu et al. introduced an environmentally friendly, non-fluorinated method for stainless steel modification. By vacuum vapor deposition technique with substitution reaction, they successfully constructed a superhydrophobic surface with dendritic layered structure on the surface of stainless

DOI: 10.54254/2755-2721/2025.29501

steel mesh. This method does not require the use of fluorine-containing materials, thus avoiding environmental pollution. At the same time, the preparation process is simple and easy to control. The prepared superhydrophobic surface has excellent anti-fouling and anti-corrosion properties. Water droplets and dirt are difficult to adhere to its surface, and corrosive ions are also difficult to penetrate. This provides a new idea for the anti-fouling and anti-corrosion of stainless-steel surfaces and is expected to be widely used in various fields [42].

4.4. Discussions on fabrics

As introduced in the previous text, although these materials are currently the mainstream, they still face some challenges. Therefore, we will further discuss the three most significant aspects that affect their practical and widespread application, and attempt to propose possible solutions to the current problems.

4.4.1. Material performance enhancement

The enhancement of material performance is crucial for promoting the application of non-fluorinated superhydrophobic/anti-fouling materials. The commonly used non-fluorinated superhydrophobic/anti-fouling materials in the market primarily include silicone materials (PDMS), organic materials, and inorganic materials. It is necessary to develop new materials with higher surface energy and hydrophobicity in the future. In future, it is essential to design new materials with higher surface energy and hydrophobicity. For example, creating micro/nano hierarchical surfaces can strongly increase the material's surface area and reduce surface energy, thus enhancing its superhydrophobic/anti-fouling performance. For example, the construction of micro/nano layered surfaces can effectively increase the surface area of the material and reduce the surface energy, thus improving the superhydrophobic/antifouling performance of the material. In addition, the combination of different types of materials can give full play to their respective advantages and improve the comprehensive performance of the materials. For example, combining silicone materials with organic or inorganic materials can combine the low surface energy of silicone with the mechanical strength of organic or inorganic materials to produce superhydrophobic/fouling-resistant materials with superior performance.

4.4.2. Durability

Despite the excellent superhydrophobic properties of these materials, their durability may be affected by environmental factors. For example, prolonged exposure to sunlight or harsh climatic conditions may lead to degradation of material properties. To improve the durability of the materials, the chemical stability and mechanical strength of the materials can be investigated to increase their resistance to environmental factors. For example, the addition of cross-linking agents, coating techniques and other technologies is an effective way to improve the strength and chemical stability of materials and enhance their durability.

4.4.3. Reducing material costs

Reducing material costs is an important way to promote the large-scale application of fluorine-free superhydrophobic/antifouling materials. Currently, the high cost of raw materials for some fluorine-free superhydrophobic/antifouling materials limits their large-scale application. Therefore, the development of low-cost raw materials that can be widely applied is also the direction of future

DOI: 10.54254/2755-2721/2025.29501

industry progress. For example, low-cost non-fluorinated superhydrophobic/anti-fouling materials can be produced by recycling waste plastics, rubbers, and other materials. Renewable energy sources and industrial waste materials can reduce costs under appropriate conditions. Renewable energy sources and industrial waste materials can effectively reduce costs under suitable conditions.

5. Limitations and outlook

5.1. Existing defects and research progress

The future holds great promise for non-fluorinated stain-repelling materials. In previous studies, these materials and techniques have been applied to a variety of fields. From raincoats to the coating on building surfaces, non-fluorinated stain-resistant layers have the potential to be utilized in a multitude of applications. These materials are particularly beneficial due to their non-toxic impact on the environment and organisms.

And nylon fibers have a promising application as an excellent DWR material. The introduction of a dendritic polymer surface structure into the fabric material enhances the water repellence of the hyperbranched polymer structure. The highly customizable and durable nature of the coatings makes them suitable for a wide range of fibers and can be used in all aspects of daily life. In the case of pine-needle Zn/ZnO coatings, for example, the unique surface structure gives the material exceptional corrosion resistance, which significantly extends its service life. Therefore, it is expected that superphosphorophobic surfaces will be fabricated in the future that will be valuable in daily life and industrial applications [3].

5.2. Research trend and application prospect

Despite the significant advancements in non-fluorinated superhydrophobic and stain-resistant materials, challenges remain, such as improving material performance, enhancing durability, and reducing costs. Future research and development efforts are needed to explore new materials and technologies, including those with higher surface energy and hydrophobicity, more durable coatings, and lower-cost raw materials, to promote large-scale application.

Acknowledgement

Yueru Li, and Zizhen Lei contributed equally to this work and should be considered co-first authors.

Author contribution

Zizhen Lei: Writing-original draft, Writing-review & editing, Investigation, Project administration, Visualization, methodology. Yueru Li: Writing-original draft, Formal analysis, Conceptualization, Data curation, Visualization, Project administration. Yuanbin Wang: Writing-original draft, Fromal analysis, Visualization

References

[1] Liu, F. & Grainger, D. W. C. FLUORINATED BIOMATERIALS.
[2] Wan Ikhsan, S. N. et al. Superwetting materials for hydrophilic-oleophobic membrane in oily wastewater treatment. Journal of Environmental Management 290, 112565 (2021).
[3] Guo, W., Li, Z. & Ma, Z. Review of Non-Fluorinated Durable Water Repellent and Stain-Resistant Materials and Their Future development. J. Phys.: Conf. Ser. 1904, 012010 (2021).

DOI: 10.54254/2755-2721/2025.29501

[4] Han, J. et al. Chemical Aspects of Human and Environmental Overload with Fluorine. Chem. Rev. 121, 4678–4742 (2021).
[5] Trager, R. A persistent perfluorinated problem.
[6] Buck, R. C. et al. Perfluoroalkyl and polyfluoroalkyl substances in the environment: Terminology, classification, and origins. Integr Environ Assess Manag 7, 513–541 (2011).
[7] Kreissig, J. PFAS and fluorine-free alternatives in lubricants and construction products - use, emissions and socioeconomic analysis of a Reach-restriction.
[8] Whiting, R. et al. (2024) PFAS and fluorine-free alternatives in lubricants and construction products. The Danish Environmental Protection Agency, ISBN: 978-87-7038-527-5
[9] Schellenberger, S. et al. Facing the rain after the phase out: Performance evaluation of alternative fluorinated and non-fluorinated durable water repellents for outdoor fabrics. Chemosphere 193, 675–684 (2018).
[10] Allahdini, A., Jafari, R. & Momen, G. Transparent non-fluorinated superhydrophobic coating with enhanced anti-icing performance. Progress in Organic Coatings 165, 106758 (2022).
[11] Kwok, D. Y. & Neumann, A. W. Contact angle measurement and contact angle interpretation. Advances in Colloid and Interface Science 81, 167–249 (1999).
[12] Roura, P. & Fort, J. Local thermodynamic derivation of Young's equation. Journal of Colloid and Interface Science 272, 420–429 (2004).
[13] surface Tension | Measurements. https: //www.biolinscientific.com/measurements/surface-tension.
[14] Hydrophobic behaviour of non-fluorinated sol–gel based cotton and polyester fabric coatings - Claudio Colleoni, Emanuela Guido, Veronica Migani, Giuseppe Rosace, 2015. https: //journals.sagepub.com/doi/10.1177/1528083713516664.
[15] Avrămescu, R.-E., Ghica, M. V., Dinu-Pîrvu, C., Prisada, R. & Popa, L. Superhydrophobic Natural and Artificial Surfaces—A Structural Approach. Materials 11, 866 (2018).
[16] Wang, K., Shen, Y., Duan, M., Wu, T. & Zhao, J. Non-fluorinated durable water repellent and stain resistant coating. (2023).
[17] C., A., S., S. A. & Mayavan, S. Salvinia inspired fluroine free superhydrophobic coatings. Applied Surface Science 449, 250–260 (2018).
[18] The impact of raindrops on Salvinia molesta leaves: effects of trichomes and elasticity | Journal of The Royal Society Interface. https: //royalsocietypublishing.org/doi/10.1098/rsif.2021.0676.
[19] Hu, D. L., Chan, B. & Bush, J. W. M. The hydrodynamics of water strider locomotion. Nature 424, 663–666 (2003).
[20] Water-repellent legs of water striders | Nature. https: //www.nature.com/articles/432036a#Bib1.
[21] Yin, Q. et al. 3D-Printed Bioinspired Cassie–Baxter Wettability for Controllable Microdroplet Manipulation. ACS Appl. Mater. Interfaces 13, 1979–1987 (2021).
[22] Surface Structure and Wetting Characteristics of Collembola Cuticles. PLOS ONE 9, e86783 (2014).
[23] Wang, K. et al. Non-fluorinated durable water repellent and stain resistant coating. Applied and Computational Engineering 7, 438–452 (2023).
[24] Huang, H.-C., Ren, Z., Chan, C. & Li, X. Wet etch, dry etch, and MacEtch of β-Ga2O3: A review of characteristics and mechanism. Journal of Materials Research 36, 4756–4770 (2021).
[25] Kota, A. K., Choi, W. & Tuteja, A. Superomniphobic surfaces: Design and durability. MRS Bull. 38, 383–390 (2013).
[26] Alhalaili, B., Vidu, R., Mao, H., Kamoun, O. & Saif Islam, M. Photoelectrochemical (PEC) etching of Ga2O3. Ceramics International 47, 479–486 (2021).
[27] Phan, N. B. & Moronuki, N. 2305 Fabrication of High Aspect Ratio Nanostructure with Metal Assisted Chemical Etching and Surface Modification Aiming at Self-cleaning Function. LEM21 2015.8, _2305-1_-_2305-4_ (2015).
[28] Liu, T. et al. Biomedical Applications of Layer-by-Layer Self-Assembly for Cell Encapsulation: Current Status and Future Perspectives. Adv Healthcare Materials 8, 1800939 (2019).
[29] Ye, J.-R., Chen, L., Zhang, Y., Zhang, Q.-C. & Shen, Q. Turning the chitosan surface from hydrophilic to hydrophobic by layer-by-layer electro-assembly. RSC Adv. 4, 58200–58203 (2014).
[30] Coatings | Free Full-Text | Robust Super-Hydrophobic Coating Prepared by Electrochemical Surface Engineering for Corrosion Protection. https: //www-mdpi-com-s.sslvpn.ecust.edu.cn: 8118/2079-6412/9/7/452.
[31] Jain, R. & Pitchumani, R. Facile Fabrication of Durable Copper-Based Superhydrophobic Surfaces via Electrodeposition. Langmuir 34, 3159–3169 (2018).
[32] Laad, M. & Ghule, B. Fabrication Techniques of Superhydrophobic Coatings: A Comprehensive Review. physica status solidi (a) 219, 2200109 (2022).

DOI: 10.54254/2755-2721/2025.29501

[33] Scalise, E., Iordanidou, K., Afanas'ev, V. V., Stesmans, A. & Houssa, M. Silicene on non-metallic substrates: Recent theoretical and experimental advances. Nano Res. 11, 1169–1182 (2018).
[34] Kong, M., Wu, Y., Men, D., Ding, Q. & Zhang, H. Preparation of hydrophobic porous Au–Ag alloy nanoparticle arrays and their SERS properties. RSC Adv. 13, 36181–36187 (2023).
[35] Barthwal, S. & Barthwal, S. A highly robust, non-fluorinated, and economical PDMS-based superhydrophobic flexible surface with repairable and flame-retardant properties. Journal of Applied Polymer Science 140, e53766 (2023).
[36] Wang, W. et al. Direct Laser Writing of Superhydrophobic PDMS Elastomers for Controllable Manipulation via Marangoni Effect. Advanced Functional Materials 27, 1702946 (2017).
[37] Wu, Y. Designing superhydrophobic robotic surfaces: Self-cleaning, high-grip impact, and bacterial repelling. (2021).
[38] Korczeniewski, E. Are nanohedgehogs thirsty? Toward new superhydrophobic and anti-icing carbon nanohorn-polymer hybrid surfaces. Chemical Engineering Journal (2022).
[39] Pinheiro, R. A. Vertically aligned carbon nanotubes (VACNT) surfaces coated with polyethylene for enhanced dew harvesting. (2020).
[40] Cui, C. Photocatalytic superhydrophobic SH-ZnO-PDMS-coated fabric for efficiency self-cleaning and oily water separation. J. Coat. Technol. Res.
[41] Li, R. A pine needle-like superhydrophobic Zn/ZnO coating with excellent mechanochemical robustness and corrosion resistance. (2023).
[42] Xu, S. Fabrication of hierarchical structures on steel mesh with good superhydrophobicity and anti-corrosion property. (2020).